

CHARACTERIZATION OF A TUBULAR HOT-CAVITY SURFACE IONIZATION SOURCE*

Y. Liu[#], Y. Kawai, H. Z. Bilheux, ORNL, Oak Ridge, TN 37831-6368, U.S.A.

Abstract

A hot-cavity surface ionization source with a cylindrical cavity having a small inner diameter, d , and a length $l \gg d$ was studied. Measured ionization efficiencies for Sr, In and Al were higher than expected from surface ionization by a factor of 20, 50, and 200, respectively. The ionization mechanism based on a thermal plasma inside the hot cavity was used to explain the results.

INTRODUCTION

Surface ionization sources have been widely used at isotope separator on-line radioactive ion beam facilities for producing ion beams of elements with ionization potentials < 6 eV because of their high efficiency, intrinsic elemental selectivity, and simplicity [1]. The concept of surface ionization involves the ionization of a low ionization potential element (W_i) on a high work function surface (Φ) hot enough to desorb the ions thermally. The degree of ionization, α , is given by the Saha-Langmuir equation

$$\alpha = \frac{n_i}{n_0} = \frac{\omega_i}{\omega_0} \exp\left(\frac{\Phi - W_i}{kT}\right) \quad (1)$$

$$\beta = \frac{\alpha}{1 + \alpha} \quad (2)$$

where β is the surface ionization efficiency, n_i and n_0 are the ion and neutral concentrations, ω_0 and ω_i are the statistical weights of the atomic and ionic states, k is the Boltzmann's constant, and T is the temperature of the surface. It has been experimentally observed that the ionization efficiency in a hot-cavity can be significantly higher than expected for the surface ionization mechanism [2,3]. This has been attributed to the existence of a thermal plasma inside the cavity consisting of surface ionized ions and thermionic electrons [4-6]. If the plasma is in quasi-neutral condition and in thermal equilibrium with the cavity wall, the ionization efficiency, η , is described by the Eggert-Saha thermal ionization formula

$$\gamma = \frac{2\omega_i}{\omega_0} \left(\frac{2\pi m_e}{h^2}\right)^{3/2} \frac{(kT)^{5/2}}{P} \exp\left(\frac{-W_i}{kT}\right) \quad (3)$$

$$\eta = \left(\frac{\gamma}{1 + \gamma}\right)^{1/2} \quad (4)$$

where m_e is the mass of electron, h is the Plank's constant, and $P = kT(n_0 + n_i + n_e)$ is the plasma pressure, n_i , n_0 and n_e being the ion, neutral and electron concentrations, respectively. In this case, the 'thermal' ionization

efficiency can be orders of magnitude higher than that of surface ionization. However, it is argued that the thermal equilibrium requirement is rarely achieved inside hot-cavities with low plasma densities [6], and thus Eq. (3) and Eq. (4) are not valid. On the other hand, due to multiple wall collisions in the hot-cavity, the atoms have a larger chance to be ionized and, once ionized, the ions can be trapped by the thermal plasma. Therefore, the enhancement in ionization efficiency is interpreted in terms of an amplification factor, $N \leq \nu$, ν being the mean number of wall collisions of atoms in the cavity [6].

$$\alpha_c = N\alpha \quad \beta_c = \frac{\alpha_c}{1 + \alpha_c} \quad (5)$$

A tubular hot-cavity surface ionization source was constructed and tested to study the ionization efficiencies for several elements of interest. We describe the ion source and report the ionization efficiencies.

DESCRIPTION OF THE SOURCE

The ion source and associated target reservoir and vapor transport system are shown in Fig. 1. The hot cavity ionizer is a 30 mm long tube having a 3 mm inner diameter and a 1 mm wall thickness. The inner diameter, d , and length, l , of the cavity are chosen such that $l \gg d$. High work function refractory materials such as W and Ta are tested as the ionizer material. Sample materials are introduced into the target reservoir, which is radiatively heated using a cylindrical Ta heater for sample vaporization. The atomic species of interest effuse through the vapor transfer line into the hot cavity where they are ionized by surface ionization. Ions are extracted from the cavity and accelerated to an energy of 20 keV. The cavity and the transfer tube are resistively heated to temperatures exceeding 2000°C. The direction of the DC electrical heating current also produces an axial electric field in the ionizer which pushes the ions towards the extractor.

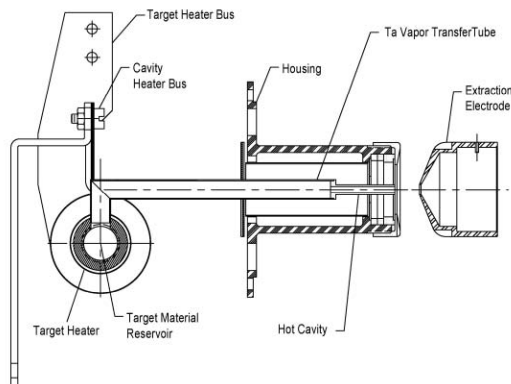


Fig. 1. Schematic drawing of the hot-cavity ion source.

*Research sponsored by the U.S. Department of Energy, under contract DE-AC05-00OR22725 with UT-Battelle, LLC.

[#]liuy@ornl.gov

OPERATION OF THE SOURCE

Thermal analysis on the source is performed with the finite element code ANSYS [7]. An axial-symmetric model of the source created using ANSYS is illustrated in Fig. 2. Although the target reservoir and the transport tube are mechanically attached, thermal coupling between them is not significant. Therefore the target reservoir is not included in the thermal analysis. Fig. 2 shows the calculated temperature distribution in the source when 400 A electrical current is applied to heat a Ta ionizer. As noted, the temperature along the cavity is not uniform. Near the middle of the ionizer has the maximum temperature, but near the exit aperture the temperature is more than 400°C cooler, because of conduction from the molybdenum housing at a much lower temperature. The position of the maximum temperature shifts toward the exit aperture with increasing heating current.

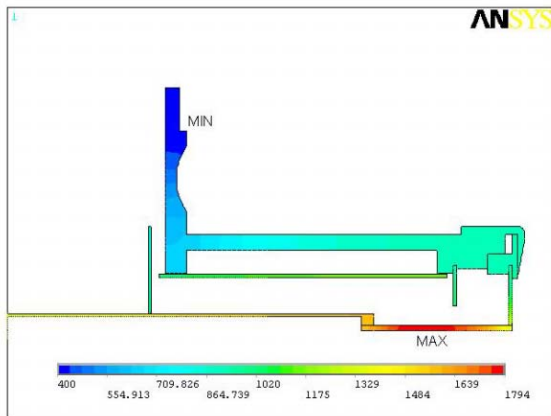


Fig. 2. Calculated temperature distribution in the source resulting from 400A heating electrical current.

The simulation results are compared with experimental observations. Fig. 3 shows the measured temperatures plotted as a function of the heating electrical current passing through the ionizer and transfer tube. The data are obtained with C-type thermocouples at two positions of the ion source: 1). the ionizer cavity, ~10 mm from the exit aperture, and 2). the vapor transfer tube at a distance of ~40 mm from the cavity. The target reservoir was not heated for these measurements. It is seen that the measured temperature at 400 A is about 200°C higher than the calculated maximum ionizer temperature. However, the temperature difference between the cavity and the transfer tube agrees with the model. Additional experimental observations also confirm that the temperature profile of the ionizer cavity is in good agreement with the thermal analysis.

SOURCE PERFORMANCE

Ion Intensity versus Heating Current

The source is characterized by feeding Cs vapor from an external oven. The oven is connected to the target reservoir via a coaxial vacuum feed-through and a small Ta vapor feed tube between the vacuum feed-through and

the target reservoir. The diameter of the feed line tube is chosen to conduction limit the flow rate of the Cs vapor.

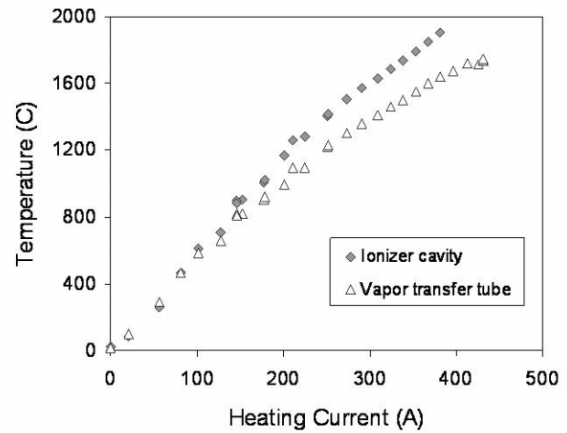


Fig. 3. Source temperature versus heating current.

The Cs oven is maintained at a constant temperature of 100°C, while the external and internal vapor feed lines are heated and kept at 250°C and 300°C, respectively. Thus, the Cs flow rate through the vapor feed line into the ionizer cavity was constant. In Fig. 4, the Cs⁺ currents extracted from the ion source and measured with a Faraday cup after a 90° dipole magnet mass separator are plotted versus the heating electrical current. The plateaus seen in the ion currents are reproducible. W ($\Phi = 4.54$ eV) has a higher work function than Ta ($\Phi = 4.25$ eV). As expected, the onset of Cs⁺ intensity occurs at a lower heating current for a W ionizer than that of a Ta ionizer, and W ionizers have, in general, higher Cs⁺ yields than Ta. However, above 450 A, the performances of Ta and W ionizers are about the same, as noted in Fig. 4. The ionization efficiency for Cs is about 92% at 500 A for both Ta and W cavities, estimated according to the Cs vapor pressure in the Cs oven, the source pressure in the ionizer cavity, and the conductance of the vapor feed line.

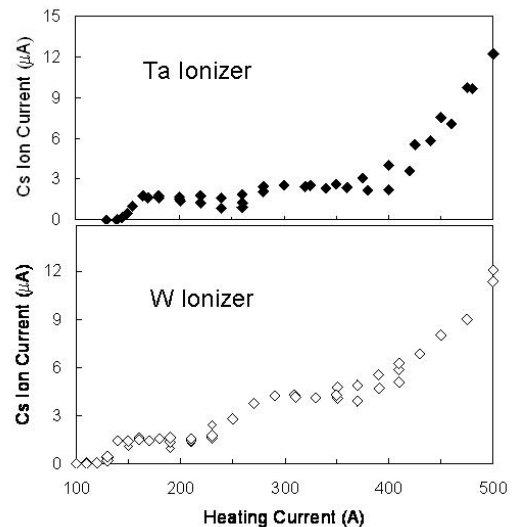


Fig. 4. Measured Cs⁺ ion currents as a function of the ionizer heating current.

The dependence of ion intensity on the heating current shown in Fig. 4 may be due to the non-uniform temperature distribution in the ionizer and limited penetration of the extraction field. At low heating currents, ions are generated in the back of the ionizer where the hot-spot is located. Only a small fraction of the ions are able to drift to the exit aperture and then extracted by the acceleration field. As the heating current is increased, the overall ionizer temperature increases and the hot-spot shifts toward the exit aperture. As a result, more ions are generated near and can reach the region where the extraction field penetrates into the cavity. Thus, the extracted ion current increases rapidly. To improve the temperature uniformity in the ionizer, a double heating path was added to half of the ionizer cavity, starting from the exit aperture. A comparison of Cs⁺ currents obtained with the original and the modified ion source equipped with a Ta ionizer is shown in Fig. 5. Note the onset of each plateau indeed shifts to lower heating current for the modified source.

The emittance of the source has been measured using a slit-grid emittance measurement system. Emittance values on the order of 10 π mm-mrad at the 90% contour level for 20 keV Cs⁺ ion beams are typical for the source. These are very small emittances in comparison with other types of ion sources.

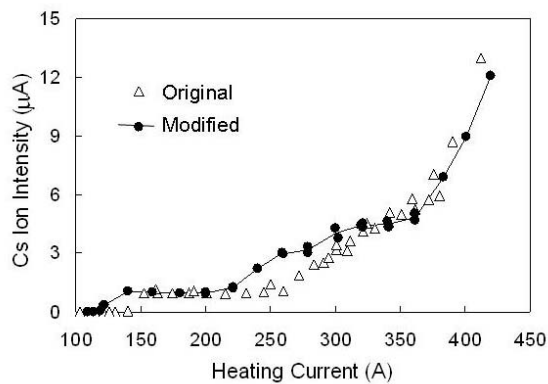


Fig. 5. Comparison of Cs⁺ currents obtained with the original source and the modified source with partial double heating path for the ionizer.

Ionization Efficiency

Ionization efficiencies for Cs, Rb, Sr, In, and Al were measured using calibrated liquid samples containing $\sim 10^{17}$ atoms per sample. For these measurements, the source was heated quickly to heating currents near or above 400 A (Fig. 4), then, samples placed in the target reservoir were heated to high temperatures for vaporization, while the ion currents were continuously recorded until the samples completely evaporated out of the source. The ionization efficiencies were calculated as the ratio of the integrated total number of detected ions to the total number of atoms in the samples. Liquid samples used are CsBr, RbBr and SrI₂ dissolved in water, and In and Al atomic spectroscopy standard solutions. The measured ionization efficiencies are summarized in Table 1.

Also listed in Table 1 are the calculated surface ionization efficiencies using Eq. (1) and Eq. (2) for the corresponding experimental ionizer temperature of 2100°C for Al and 2000°C for the others. The experimental efficiencies for Cs and Rb are lower than the theoretical values. This is likely due to the high volatility of the sample materials used (CsBr and RbBr) -- a large fraction of the sample molecules are lost before the ionizer cavity is hot enough to dissociate the molecules and ionize the atoms. On the other hand, the measured efficiencies for Sr, In and Al are more than a factor of 20, 50 and 200, respectively, higher than the corresponding theoretical surface ionization efficiencies.

Table 1. Ionization Efficiencies

element	IP (eV)	Measured (%)		β (%)	
		W	Ta	W	Ta
Cs	3.894	50	30	93	75.5
Rb	4.177	35	20	76	42
Sr	5.695	12.9	5.2	0.55	0.13
In	5.786	5		0.09	
Al	5.986	10.3		0.043	

The ionization mechanism described by Eq. (5) is used to explain the results. The mean number of wall collisions, ν , that a neutral particle may undergo while passing through a cylindrical tube is usually estimated as the ratio of the inner surface to the cross section area of the exit aperture [6]. Thus, $\nu \sim 40$ for a 3 mm inner diameter and 30 mm long tube. Using a Monte Carlo code [8], we get $\nu \approx 46$ if neutrals impinging on the surface are specularly reflected, and $\nu \approx 200$ if neutrals leave the wall according to the cosine law. Inserting these values for ν in Eq. (5), the observed efficiencies for Sr and In can be explained. However, for Al, the enhanced efficiency, $\beta_c = 7.8\%$ obtained assuming $N = 200$ in Eq. (5), is still lower than the experimental value.

REFERENCES

- [1] R. Kirchner, Rev. Sci. Instrum. 67 (1996) 928.
- [2] G. Beyer, E. Herrmann, A. Piotrowski, V.I. Raiko and H. Tyroff, Nucl. Instr. and Meth. 96 (1971) 437.
- [3] P.G. Johnson, A. Bolson and C.M. Henderson, Nucl. Instr. and Meth. 106 (1973) 83.
- [4] R. Kirchner and A. Piotrowski, Nucl. Instr. and Meth. 153 (1978) 291.
- [5] M. Huyse, Nucl. Instr. and Meth. 215 (1983) 1.
- [6] R. Kirchner, Nucl. Instr. and Meth. A 292 (1990) 203.
- [7] <http://www.ansys.com>.
- [8] Y. Zhang and G.D. Alton, Proceedings of the 18th International Conference on the Application of Accelerators in Research and Industry, October 10-15, 2004, Fort Worth, TX, USA.